

## Internal pressure with varying sizes of dominant openings and volumes – model studies

John Ginger and Peter Kim

*Cyclone Testing Station, James Cook University, Townsville, Queensland, Australia*

### 1. INTRODUCTION

The internal pressure can contribute a significant proportion to the total design wind loads when there is a dominant opening in the envelope of a building. Holmes [1], Vickery [2] and Ginger *et al* [3] have carried out model and full scale studies on internal pressures in nominally sealed buildings and buildings with a range of openings, and showed that results compare favorably with theoretical analysis. Design internal pressure data specified in the wind load standard AS/NZS 1170.2 [4] is based on such studies with a limited range of opening sizes and volumes. In this paper, characteristics of internal pressures in buildings, with a range of dominant opening sizes and volumes, are studied using model-scale data to determine the importance of the sizes of dominant opening area and building volume when calculating design internal pressures. Results are presented in a non-dimensional format useful for design standards.

### 2. THEORY

The external pressures ( $p_E$ ) and internal pressures ( $p_I$ ) are defined in coefficient form as:  $C_p = p / \frac{1}{2} \rho \bar{U}_h^2$  where,  $\bar{p}$ ,  $\sigma_p$ ,  $\hat{p}$  are the mean, standard deviation and maximum pressure,  $\rho$  is the density of air, and  $\bar{U}_h$  is the mean wind speed at roof height,  $h$ . Pressures acting towards a surface is defined positive. The frequency distribution of pressure fluctuations are further studied by analyzing their spectral densities, given by  $S(f)$ . The internal pressure fluctuations are related to the external pressures using the admittance function,  $|\chi_{p_I/p_E}|^2$  shown in Eq. 1, also defined as square of the gain function  $G(f)^2$ .

$$S_{p_I}(f) = |\chi_{p_I/p_E}|^2 S_{p_E}(f) = G(f)^2 S_{p_E}(f) \quad (1)$$

The relationship between mean internal pressure ( $\bar{p}_I$ ), mean external windward pressure ( $\bar{p}_W$ ) and mean external leeward pressure ( $\bar{p}_L$ ), given by Eq. 2., is used in many codes and standards (i.e. AS/NZS 1170.2 [4]) to derive quasi-steady internal pressure coefficients for given windward to leeward opening ratios  $A_W/A_L$ , in buildings.

$$C_{\bar{p}_I} = C_{\bar{p}_W} / [1 + (A_L/A_W)^2] + C_{\bar{p}_L} / [1 + (A_W/A_L)^2] \quad (2)$$

For a building with a single opening, Eq. 2. shows that the mean internal pressure is equal to the mean external pressure at the opening. Furthermore, Vickery [2] also showed that the internal pressures have negligible variation if the total background leakage is less than about 10% of the dominant opening. In such cases, a valid approach is to study the pressure in a sealed building with a single opening.

Holmes [1] derived Eq. 3, to describe the time dependent internal pressure in a building with a dominant opening of area  $A$ , in terms of internal pressure coefficient,  $C_{p_I}$  and external pressure coefficient at the opening,  $C_{p_E}$ . Here,  $p_0$  is the atmospheric pressure,  $k$  is the discharge coefficient of the opening,  $n$  is the ratio of specific heats of air, and  $l_e = \sqrt{(\pi A/4)}$  is the effective length of the “slug” of air moving in and out

of the opening.  $V_{le}$  is the effective internal volume of the building which also accounts for flexibility of the building. The speed of sound  $a_s = (n \times p_0 / \rho)^{1/2}$ , where  $n = 1.4$  for an adiabatic process. The undamped Helmholtz frequency is  $f_H = \frac{1}{2\pi} \sqrt{nAp_0 / \rho l_e V_{le}}$ .

$$\frac{\rho l_e V_{le}}{nAp_0} \ddot{C}_{p_i} + \left[ \frac{\rho V_{le} \bar{U}_h}{2nkAp_0} \right]^2 \dot{C}_{p_i} | \dot{C}_{p_i} | + C_{p_i} = C_{p_E} \quad (3)$$

Holmes [1] also showed that the internal pressure fluctuations can be represented as a function of the five non-dimensional parameters:  $\Phi_1 = A^{3/2} / V_{le}$ ,  $\Phi_2 = a_s / \bar{U}_h$ ,  $\Phi_3 = \rho \bar{U}_h \sqrt{A} / \mu$ ,  $\Phi_4 = \sigma_U / \bar{U}$  and  $\Phi_5 = \lambda_U / \sqrt{A}$ , where,  $\mu$  is the viscosity of air,  $\bar{U}$  and  $\sigma_U$  are the mean velocity and turbulence intensity respectively of the flow at a given elevation, and  $\lambda_U$  is the integral length scale of turbulence.

Eq. 3 can be written in the non-dimensional form of Eq. 4, by introducing these non-dimensional parameters, and by defining a non-dimensional time,  $t^* = t \bar{U}_h / \lambda_U$ . The first term in Eq. 4 describes the ‘‘inertia’’ of the air flow in and out of the opening, while the second term represents the damping of the flow through the opening.

$$\left( \frac{\sqrt{\pi}}{2} \right) \frac{1}{\Phi_1 \Phi_2^2 \Phi_5^2} \frac{d^2 C_{p_i}}{dt^{*2}} + \left( \frac{1}{4k^2} \right) \left[ \frac{1}{\Phi_1 \Phi_2^2 \Phi_5} \right]^2 \frac{dC_{p_i}}{dt^*} \left| \frac{dC_{p_i}}{dt^*} \right| + C_{p_i} = C_{p_E} \quad (4)$$

The product  $\Phi_1 \Phi_2^2$  in Eq. 4, can be replaced by a single non-dimensional variable and defined as the non-dimensional opening to volume parameter,  $S^* = (a_s / \bar{U}_h)^2 (A^{3/2} / V_{le})$ . Eq. 4 shows that the variation of internal pressure for given external pressure fluctuations is dependent on  $S^*$ ,  $A$  and  $k$ , and that there is a unique solution for  $C_{p_i}$  with  $S^*$ , for a given  $A$  and  $k$ . Therefore, given the value of  $k$ , the ratio of internal pressure fluctuations to external pressure fluctuations at the opening, can be presented by a family of curves, with variables of  $S^*$  and  $A$ . Eq. 4 also shows similarity is maintained by keeping  $S^*$  constant, giving the same volume distortion requirements recommended by Holmes [1], for model tests.

### 3. EXPERIMENTAL SET-UP, RESULTS AND DISCUSSION

External and internal pressures were measured on a  $200 \times 400 \times 100$  mm model building shown in Figure 1, in a boundary layer flow simulated to terrain category 2 at a length scale of 1/100, in the wind tunnel at James Cook University. The  $200 \times 400 \times 600$  mm volume located below floor level in the wind tunnel is available for varying the internal volume of the building.

External pressures were measured at 30 taps on a panel centered on the 400 mm long windward wall of the nominally sealed model building, for  $\theta = 0^\circ$  winds approach, as shown in Figure 1. Pressure measurements on selected taps are combined to give area-averaged external, mean, standard deviation and maximum  $C_p$ s on Areas A1, A2, A3 and A4 representative of potential dominant openings on the building defined in Table 1. Internal pressures measured inside the model with a dominant opening of A1, A2 A3 or A4 on the 400mm long wall, and internal volumes V1 or V7, for approach wind direction,  $\theta = 0^\circ$ , and the Helmholtz frequencies,  $f_H$  calculated for these combinations of opening sizes  $A$  and volumes  $V_{le}$  are also given in Table 1. Tests were carried out at mean approach wind speeds at roof height,  $\bar{U}_h$  of about 10 m/s. The pressure signals were sampled at 1250 Hz for a single run of 30 s duration, and data presented from the average five runs. The results indicate that the mean internal pressure closely follows the mean external pressure for each dominant opening size.

The pressure spectra,  $S_p(f)$  and admittance functions,  $G(f)^2$  obtained from measured windward wall external pressure and measured and simulated (using  $k = 0.1, 0.3$ ) internal pressures for A2, and V1 and V7 are shown in Figs. 2a and 2b, respectively. The figures show that internal pressure resonance occurs close to the Helmholtz frequency (which decreases with increase in volume), and that  $k = 0.1$  and  $0.3$  gives a satisfactory simulation of internal pressures. In accordance with Eq. 4, although a reduction in  $S^*$  (increase in  $V_{le}$ ) results in increased damping of internal pressure fluctuations, an increase in  $k$  indicates comparable peaks in  $G(f)^2$  near the Helmholtz frequency. The magnitude of internal pressure fluctuations also depends on the position of Helmholtz frequency in relation to the energy containing range of frequencies in the external pressure fluctuations, notwithstanding an increase in damping.

Standard deviation and peak (i.e. maximum), simulated ( $k = 0.3$ ) internal to windward wall external pressure ratios are shown for A1, A2, A3 and A4, as a function  $S^*$ , in Figs. 3a and 3b respectively. The measured internal to windward wall external, standard deviation pressure ratios shown in these figures are in good agreement with the simulations, but the peak internal pressures are generally overestimated by these simulations. Nevertheless, this analysis shows that the size of the opening and volume play an important part in internal pressure fluctuations, and that the magnitude of the internal pressure fluctuations increase with increasing  $S^*$ . The relationship between internal and windward wall external pressure fluctuations have similar trends to that found by Ginger et al [5], using limited full scale data. Additional secondary frequency peaks were observed on the internal pressure spectra, as the volume was increased.

#### 4. CONCLUSIONS

This study found that the characteristics of the internal pressure fluctuations are influenced by the size of the dominant opening and the size of the volume, and by the approach wind speed. The relationship between the internal pressure fluctuations and the external pressure at the dominant opening can be provided in terms of the standard deviation and peak pressure ratios versus  $S^* = (a_s/\bar{U}_h)^2 (A^{3/2}/V_{le})$ , for a range of opening sizes. The internal pressure fluctuations (standard deviation and peak) are amplified as  $S^*$  increases. Internal pressures simulated with  $k = 0.1$  to  $0.3$  provide satisfactory comparisons with measured internal pressures and internal to external pressure ratios, for a range  $S^*$ . These relationships are similar to that found with limited full-scale data by Ginger et al [5].

#### 5. REFERENCES

- 1 J. D. Holmes, Mean and fluctuating internal pressures induced by wind, Proc. 5th Int. Conf. on Wind Eng., Colorado USA, 1979, Vol. 1, pp. 435-450.
- 2 B. J. Vickery, Internal pressures and interactions with the building envelope, J. Wind Eng. & Ind. Aerodyn., 53(1994) 125-144
- 3 J. D. Ginger, K.C. Mehta, and B.B. Yeatts, Internal pressures in a low-rise full scale building, J. Wind Eng. & Ind. Aerodyn., 72(1997) 163-174.
- 4 Standards Australia, Australian/New Zealand Standard, Structural design actions. Part 2: Wind actions. AS/NZS 1170.2:2002.
- 5 J. D. Ginger, J. D. Holmes, and G. A. Kopp, Effect of building volume and opening size on fluctuating internal pressure, Wind and Structures Journal, Vol. 11, No. 5 (2008), 361-376.

Table 1. Dominant opening size ( $A$ ), internal volume ( $V_{le}$ ) Helmholtz frequency ( $f_H$ ) and measured external and internal pressure coefficients

$A$ (mm <sup>2</sup> )	$V_{le}$ (mm <sup>3</sup> )	$f_H$ (Hz)	$C_{\bar{p}E}$	$C_{opE}$	$C_{\hat{p}E}$	$C_{\bar{p}I}$	$C_{opI}$	$C_{\hat{p}I}$
A1 = 20×20	V1 = 200×400×100	91	0.52	0.21	2.10	0.56	0.23	2.06
	V7 = 200×400×700	34				0.48	0.19	1.54
A2 = 50×25	V1 = 200×400×100	121	0.53	0.21	2.04	0.57	0.20	1.85
	V7 = 200×400×700	46				0.53	0.22	1.63
A3 = 50×50	V1 = 200×400×100	144	0.55	0.22	1.98	0.59	0.23	1.82
	V7 = 200×400×700	54				0.55	0.23	1.77
A4 = 50×80	V1 = 200×400×100	162	0.52	0.20	1.89	0.54	0.20	1.64
	V7 = 200×400×700	61				0.53	0.21	1.69

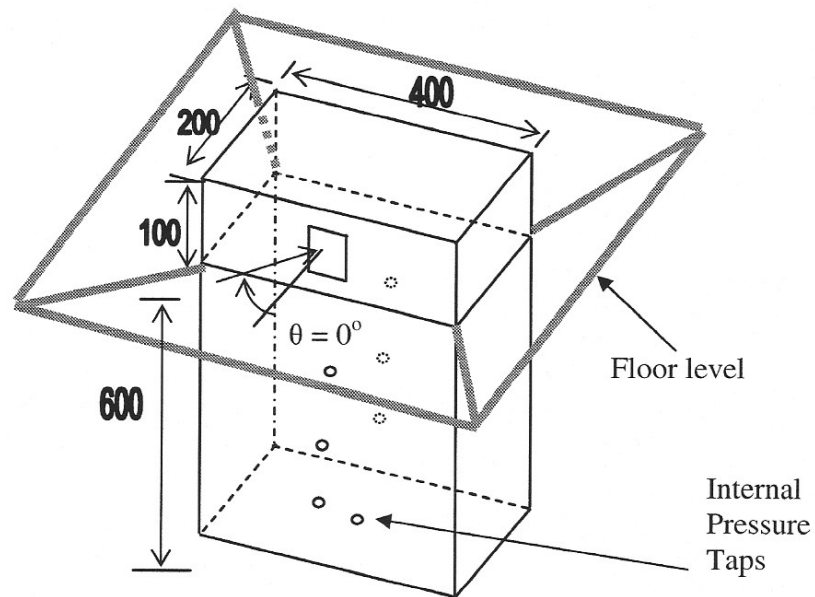


Figure 1. 200 × 400 × 100 mm model building with 200 × 400 × 600 mm volume below floor level

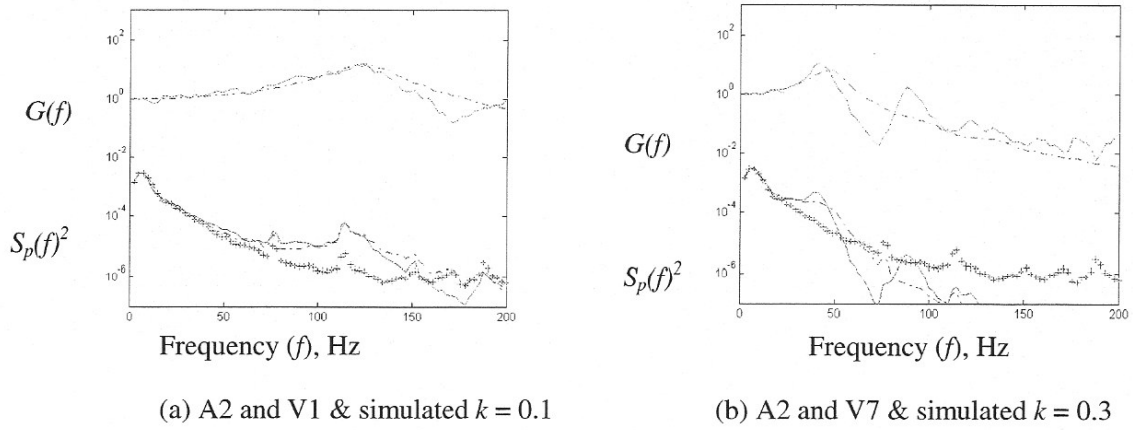


Figure 2. External (+++) and internal (measured (\_\_\_) and simulated (.\_.\_))  $S_p(f)$  and  $G(f)^2$ ,

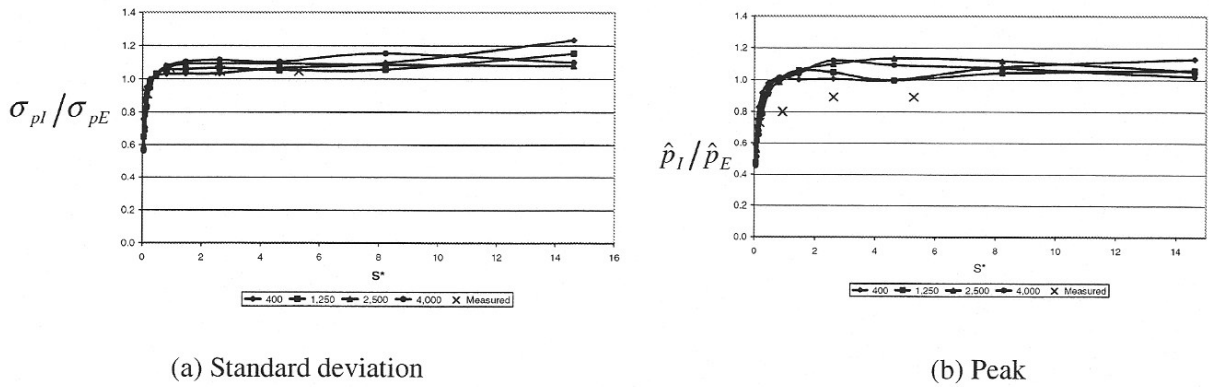


Figure 3. Pressure ratios vs  $S^*$  simulations with  $k = 0.3$ ,  $A = 400, 1250, 2500$  and  $4000 \text{ mm}^2$